Dynamics of Brain Lateralization and Genetic Underpinnings during Chinese Natural Speech Processing: Preferential Occurrence of Logic-Related Patterns in Males and Emotion-Related Patterns in Females

Ruohan Zhang[1], Shujie Geng[2,3], Xiaoqing Zheng[4], Wanwan Guo[2,3,5], Chun-Yi Zac Lo[6], Jiaying Zhang[7,8], Xiao Chang[2,3], Xinran Wu[2,3], Jie Zhang[2,3], Miao Cao[2,3*] and Jianfeng Feng[1,2,3*]

[1]Department of Computer Science, University of Warwick, Coventry, CV4 7AL, UK
[2]Institute of Science and Technology for Brain-Inspired Intelligence, Fudan University, Shanghai 200433, China
[3]Key Laboratory of Computational Neuroscience and Brain-Inspired Intelligence (Fudan University), Ministry of Education, China
[4]School of Computer Science, Fudan University, Shanghai 200433, China
[5]Shenzhen Institute of Neuroscience, Shenzhen, 518107, China
[6]Department of Biomedical Engineering, Chung Yuan Christian University, Taoyuan, Taiwan
[7]School of Artificial Intelligence, Beijing University of Posts and Telecommunications, Beijing 100876, China
[8]State Key Laboratory of Cognitive Neuroscience and Learning, Beijing Key Laboratory of Brain Imaging and Connectomics, IDG/McGovern Institute for Brain Research, Beijing Normal University, Beijing 100875, China

* Please send correspondence to: Miao Cao (mcao@fudan.edu.cn) and Jianfeng Feng (jianfeng64@gmail.com)

Abstract

Although language is considered unique to humans with left dominant lateralization in brains, the dynamic nature of the interplay between hemispheres during language processing remains largely unknown. Here, we investigated whole-brain functional dynamic lateralization patterns during Chinese language processing and potential sex disparities using functional MRI data of 20 subjects listening to narrative stories in a 7T MRI scanner. Our findings revealed two distinct dynamic lateralization states, with areas of the language system consistently exhibiting left-lateralized and converse lateralization patterns for both association areas and primary sensorimotor areas. These two states, characterized by areas of higher-order systems exhibiting left- or right-lateralization, corresponded to the processing of rational and emotional contents. We observed pronounced inclinations towards the former state in males and the latter state in females, especially during the processing of rational content. Finally, genetic analysis revealed that the sex differences in lateralization states were potentially influenced by sex hormones.

Keywords: dynamic laterality; Chinese language processing; naturalistic imaging; sex differences; dynamic functional states

Introduction

Languages are distinctively used by humans, and language processing is characterized by intricate, complex, and diverse neural mechanisms. One notable aspect of language processing is brain lateralization, as the language system was traditionally assumed to be situated mainly in the left hemisphere, enhancing efficiency in multitask performance[1,2] and reducing redundancy in neural organization[3-6]. Nevertheless, some neuroimaging studies have revealed language processing-related regions in the right hemisphere, though they are relatively marginal[7-9]. Furthermore, as a high-level cognitive function, language processing relies on information coordination across a broad range of cognitive and behavioural domains, including memory, learning, and cognitive control[10-19]. Most previous studies on language lateralization typically considered language processing a distinct module within the brain. However, the functional lateralization of language processing throughout the cortex remains largely unknown.

Moreover, lateralization has traditionally been treated as a static feature of the human brain. However, researchers have recognized that the inherent dynamic coordination of information is a fundamental requirement for optimal brain functioning, spanning both cognitive and behavioural domains[20-22]. Specifically, functional magnetic resonance imaging (fMRI) studies have revealed that language processing involves highly dynamic interactions across different brain regions[12,13,16-19]. The processing hierarchy from visual processing to working memory and core language systems during sentence recognition has been revealed with dynamic causal models[15]. Different dynamic interaction patterns between linguistic and domain-general systems during various cross-language processing operations, such as backwards and forwards translation, have also been reported[18]. Notably, by examining the dynamic properties of different brain regions within a predefined language system, researchers found that regions in the left hemisphere have stable processing functions, while those in the right hemisphere have more flexible periphery functions[23]. Nevertheless, our understanding of the dynamic functional lateralization of language processing across the entire cerebral cortex remains limited. In a recent study, Wu et al.[24] investigated dynamic lateralization in the brain in the resting state and its association with language functions and cognitive flexibility. This work suggests the potential of exploring dynamic lateralization across the whole brain during language processing.

Furthermore, sex differences have been reported for many cognitive functions, such as theory of mind[25], visual-spatial processing[26], and language processing[26-30]. Brain imaging studies have suggested sex differences in brain lateralization during language processing. For instance, a few investigations have indicated that males exhibit stronger left lateralization in the brain than females while performing language tasks[30-32], while females exhibit greater bilateral activation in language-related regions than males, including the inferior frontal gyrus, posterior superior temporal gyrus, and fusiform gyrus[26-29,33]. Nevertheless, the impact of sex on dynamic lateralization patterns throughout the brain during language processing remains largely unknown. Additionally, although studies on semantics have unveiled distinct patterns of brain activation across cortical brain regions in response to various contextual factors[34,35], the impact of these factors on dynamic lateralization, especially in the different sexes, remains unexplored.

To address these issues, we acquired fMRI data using an ultrahigh-field 7T Siemens Terra MR scanner with a cohort of 20 participants (with a mean age of 23.7 ± 1.8 years and 10 females for sex balance) while they performed a Chinese language natural listening task. During the task, all participants listened to two-hour narratives that replicated authentic language to simulate language processing in real-life situations. For the analyses, we employed a data-

driven approach that combines a sliding window technique with the global signal-based laterality index to identify recurring whole-brain dynamic lateralization states. Then, we examined the spatial and temporal properties of the states as well as influences of sex and content. Next, we explored the genetic underpinnings of the observed dynamic lateralization states with publicly available postmortem brain-wide gene expression data. Finally, using resting-state fMRI data from the Human Connectome Project (HCP) cohort, we investigated whether the properties of the dynamic lateralization states observed during the Chinese natural listening task are related to inherent lateralization patterns. Fig. 1 provides a general schema of the present study.

Results

Categories of the Chinese natural speech stimuli

Participants listened to a set of twenty 8- to 12-minute narratives covering various genres, including fairy tales, fables, novels, essays, news, and scientific essays. We utilized natural language processing techniques and hierarchical clustering analysis approaches to classify the Chinese natural speech stimuli based on their semantic information. The clustering results were visualized using a dendrogram, revealing two distinct article categories (Fig. S1a). Then, we performed an assessment to confirm the optimal number of clusters based on the silhouette criterion[36]. This evaluation affirmed the suitability of classifying articles into two categories, as indicated by the highest silhouette value (Fig. S1b). Subsequently, we manually labelled one category as articles with an emotional narrative tone (12 articles) and the other as articles with a rational narrative tone (8 articles) (see Table 1 for details). These labels were used to investigate the influence of the type of content on brain dynamic lateralization patterns.

Two distinct dynamic lateralization states associated with rational and emotional text processing

We employed an approach combining a sliding window technique and the global signal-based laterality index to calculate the dynamic laterality index (DLI) of the 426 brain regions in the HCPex atlas[37]. The group-averaged laterality maps across all time windows are shown in Fig. 2a. Most left hemisphere brain regions showed left lateralization, except for specific regions in the visual cortex, paracentral lobule, middle cingulate, and posterior cingulate, which showed slight right lateralization. In contrast, nearly all right hemisphere regions displayed right lateralization, except for some auditory association areas (such as the STG area), which exhibited relatively neutral laterality (Fig. 2a).

By employing a two-stage temporal clustering approach based on the Louvain community detection algorithm[38], we identified two recurring whole-brain dynamic lateralization states with distinct brain lateralization patterns (Figs. 2b and 2c). In both dynamic lateralization states, most brain regions consistently exhibited lateralization towards the hemisphere they belong to. Specifically, in State 1, the left hemisphere regions such as the dorsolateral prefrontal cortex and inferior parietal cortex (such as area 45) exhibited strong left lateralization (Fig. 2b). In State 2, right hemisphere regions such as the dorsolateral prefrontal cortex, posterior cingulate cortex, and inferior parietal cortex displayed pronounced right lateralization (Fig. 2c). However, we observed a distinct reversal of the typical lateralization pattern in certain brain regions in these two states, such as the somatosensory cortex, the paracentral lobule, and the middle

cingulate cortex. In State 1, these left hemisphere regions exhibited right lateralization, whereas in State 2, these right hemisphere regions displayed left lateralization.

To elucidate the properties of these two states, we investigated their potential differences with respect to text sentiment. We segmented all the audio files into sentences using natural language processing (NLP) techniques and then manually assigned the sentiment score to each sentence. Specifically, sentences with rational contents were labelled 0, and those with emotional contents were labelled 1. After aligning the time windows of the fMRI data with the audio data, we determined the sentiment score for each time window and averaged the scores for each state. The average sentiment score for State 1 was 0.29, which was significantly lower than that for State 2, with an average score of 0.32 ($t = -3.3$, $p = 9.6\times10^{-4}$). According to the predefined criteria for sentiment labelling of the audio data, we classified State 1 as the dynamic lateralization state associated with the processing of rational contents, while State 2 was characterized as the dynamic lateralization state associated with the processing of emotional contents.

Spatial organization and cognitive functions of the two dynamic lateralization states

To investigate the spatial organization of the two dynamic lateralization states, we conducted a spatial community analysis for each state using the Louvain community detection algorithm[38] (Fig. 3a). State 1 exhibited five distinct spatial communities, while State 2 displayed four. To ensure cross-state comparability among these communities, we aligned them by reassigning labels based on their anatomical locations.

To elucidate the cognitive functions associated with the spatial organization of these two states, we employed a predefined cognitive component template[39] to characterize the cognitive functions associated with each community. In both states, Community 1 (C1), primarily associated with language processing, was predominantly located in the left hemisphere. Notably, C2 represented a cluster of regions responsible for higher-order cognitive functions, such as theory of mind, flanker tasks, and reward processing. Additionally, C3, which was related to lower cognitive processes such as visual processing and saccades, consistently displayed balanced lateralization between both hemispheres in both states. Furthermore, C4 was associated with sensory and motor processing. The C5 community was only observed in State 1 and was primarily located within subcortical regions involved in sensory and motor processing.

To quantify the communities in the two states which were aligned, we employed a community transition rate (CTR) matrix to assess how communities are segmented and integrated during state transitions. Overall, C1 and C4 occupied a large proportion of brain regions in State 1, but in State 2, the proportions of brain regions distributed among the four communities were relatively balanced (Fig. 3b). When transitioning from State 1 to State 2, C1 and C4 in State 1 were segmented and subsequently integrated into other communities in State 2. On the other hand, C2 and C3 remained relatively stable during the state transition, with most brain regions remaining within their respective communities. In State 2, C2, primarily associated with higher-order cognitive functions, included the five communities observed in State 1. More specifically, C2 in State 2 included all of C2, 37% of C4, 26% of C1, 9% of C3, and 8% of C5 from State 1. In addition, C4 in State 2, involved in reward processing and sensory functions, included half of the brain regions from C4 in State 1 and nearly all of C5 from State

1. Conversely, during the transition from State 2 to State 1, the communities underwent reverse segmentation and integration processes.

The mean DLI values for the communities in these two states are displayed in Fig. 3c, showing a significant contrast between the two states. In State 1, left-lateralized regions were primarily associated with higher-order cognitive functions, such as reward processing, theory of mind, and flanker tasks, and the right-lateralized regions were primarily responsible for primary functions, such as saccades and sensory, motor and visual processing. However, the regions in State 2 exhibited different patterns. Notably, C4, associated with sensory and motor processing, was predominantly localized to the right hemisphere in State 1 but displayed a nearly balanced distribution across both hemispheres, especially in subcortical regions, in State 2. This shift may be related to the higher prevalence of emotion processing observed in State 2.

Moreover, we computed the mean activation values for the communities in both states (Fig. 3d). In State 1, the activation values of the five communities considerably varied, with significant differences in activation observed between every pair of communities after Bonferroni correction ($p < 0.05/10$). Specifically, C4, related to sensory and motor processing, exhibited the highest activation, followed by C2, which was associated with theory of mind, flanker tasks, and reward processing. In State 2, the activation value of the four communities were relatively balanced, yet significant differences in activation were still observed after Bonferroni correction ($p < 0.05/6$). Additionally, communities associated with higher-order functions (C1 and C2) displayed greater activation values than those involved in lower-order cognitive processes (C3 and C4).

Differences in the temporal properties of dynamic lateralization states and influences of sexes and content types

We examined the disparities in the temporal properties of the two lateralization states, including the occurrence rate, mean dwell time, and transition probability, using a linear mixed-effects model. We also investigated the influences of both sex and content (emotional or rational) on these temporal properties and the lateralization of the states. First, we found that the occurrence rate was significantly higher in State 2 than in State 1 (mean of State 1 = 48.2%, mean of State 2 = 51.8%, $p = 1.9\times10^{-3}$) (Fig. 4a). Moreover, sex differences had considerable impacts on the occurrence rates in both states. In State 1, males exhibited significantly higher occurrence rates than females (mean of males = 50.2%, mean of females = 46.1%, $p = 6.0\times10^{-3}$). Further analysis revealed that this disparity primarily occurred when participants were presented with articles with rational contents (mean of males = 52.0%, mean of females = 46.4%, $p = 0.02$), and no significant sex differences were observed when participants were presented with articles with emotional contents. Conversely, in State 2, females displayed significantly higher occurrence rates than males (mean of males = 49.8%, mean of females = 53.9%, $p = 6.0\times10^{-3}$), and this difference was also associated with the presentation of rational articles (mean of males = 48.0%, mean of females = 53.6%, $p = 0.02$). Additionally, no significant differences in the occurrence rate were observed between content types for either state.

Furthermore, the mean dwell time was significantly longer in State 2 than in State 1 (mean of State 1 = 15.6, mean of State 2 = 16.9, $p = 0.02$) (Fig. 4a). This difference was particularly pronounced in females (emotional articles: mean of State 1 = 14.2, mean of State 2 = 17.0, $p = 1.0\times10^{-4}$; rational articles: mean of State 1 = 15.5, mean of State 2 = 18.2, $p = 8.4\times10^{-3}$) (Figs. 4d and 4e). Furthermore, sex differences were observed only in State 1 (mean of males = 16.4,

mean of females = 14.7, p = 0.02). No significant differences in mean dwell time were observed between content types for either state (Figs. 4b and 4c).

The transition probability from States 1 to 2 was significantly higher than that from States 2 to 1 (mean of States 1 to 2 transition = 0.076, mean of States 2 to 1 transition = 0.070, p = 0.01) (Fig. 4a). This difference was observed only in females during the processing of emotional articles (mean of States 1 to 2 transition = 0.080, mean of States 2 to 1 transition = 0.066, p = 6.0×10-4) and rational articles (mean of States 1 to 2 transition = 0.078, mean of States 2 to 1 transition = 0.065, p = 0.01) (Fig. 4d and 4e). No differences in transition probabilities were observed in males. Furthermore, sex differences were found in the transition probability from States 2 to 1, with the transition probability significantly lower in females than in males (mean transition probability of females = 0.066, mean transition probability of males = 0.075, p = 2.1×10-3). This difference was observed when participants were presented with either emotional (mean transition probability of females = 0.066, mean transition probability of males = 0.073, p = 0.04) or rational articles (mean transition probability of females = 0.065, mean transition probability of males = 0.079, p = 0.01). No sex differences were found in the transition probability from States 1 to 2. Additionally, no significant differences in transition probabilities were observed between content types for either state.

Significant sex differences in laterality fluctuation (LF) were particularly evident during the processing of rational articles. In State 1, these differences were primarily observed in specific brain regions, including the somatosensory and motor cortices (such as areas 1 and 3), the medial prefrontal cortex (such as areas a24 and p24), which is associated with theory of mind, the posterior cingulate cortex, which is associated with episodic memory (such as areas 31a and 31pd), the medial temporal cortex (such as parahippocampus), the emotion-related insular cortex (region Pir) and the amygdala (Fig. 5a). In State 2, the brain regions exhibiting significant differences in LF were similar to those in State 1, primarily involving the somatosensory and motor cortices, anterior insular cortex, amygdala, dorsolateral prefrontal cortex, and inferior parietal cortex (Fig. 5b). Additionally, only one region in the insular cortex in the right hemisphere (i.e., area PoI1) showed significant sex differences in LF during the processing of emotional articles (Fig. S2). Furthermore, it is noteworthy that males generally exhibited higher LF values in all these brain regions, displaying sex differences in LF.

Gene set enrichments for dynamic lateralization states

To explore the genetic underpinnings of the two dynamic lateralization states, we conducted a gene set enrichment analysis of the two states. Correlation analyses between gene expression and dynamic lateralization states showed significant associations with State 1 and State 2, and we identified 4,080 and 3,355 genes with significant correlations in States 1 and 2, respectively. These identified genes were associated with specific mental disorders, cognitive functions, and hormones, particularly sex hormones, based on the gene sets from the GWAS Catalog[40].

More specifically, significant enrichment of genes associated with specific mental disorders, such as neuroticism (q value=7.1×10^{-5}), schizophrenia (q value=2.4×10^{-4}), and autism spectrum disorder (q value=0.01), was observed in State 1. Furthermore, significant enrichment of genes associated with specific cognitive functions, including general risk tolerance (q value=5.1×10^{-7}), cognitive ability (q value=1.2×10^{-3}), and educational attainment (q value=0.01), was observed in State 1. Intriguingly, significant enrichment of genes related to hormones, notably male sex hormones, encompassing traits such as chronotype (q

value=5.1×10^{-7}), sleep duration (q value=4.8×10^{-3}), and male-pattern baldness (q value=0.03), was also observed in State 1 (Fig. 6a).

In contrast, different gene enrichment patterns were observed in State 2 than in State 1. In addition to genes associated with mental disorders (such as bipolar disorder, q value=1.4×10^{-4}) and cognitive functions (such as intelligence, q value=0.02), enrichment of genes associated with inflammatory bowel diseases, specifically Crohn's disease (q value=3.3×10^{-3}), was observed in State 2. Interestingly, significant enrichment of genes associated with female sex hormones, including menarche (q value=0.03) and breast cancer (q value=0.04), was also observed in State 2 (Fig. 6b).

Similarities in dynamic lateralization states between the resting state and Chinese natural speech task

To investigate whether the dynamic lateralization states identified during the Chinese natural listening task represent inherent lateralization patterns during resting state within the human brain, we conducted an analysis of dynamic brain lateralization using resting-state fMRI data collected from a sample of 991 participants enrolled in the HCP cohort (mean age 28.7 ± 3.7 years, 528 females). Three distinct dynamic lateralization states were identified during the resting state, as shown in Fig. S3. Interestingly, two of these states exhibited significant similarities with the two dynamic lateralization states identified during the processing of Chinese natural speech stimuli (for State 1, r=0.79, p=6.4×10^{-79}; for State 2, r=0.79, p=5.3×10^{-79}). This implies that the two dynamic lateralization states observed during the processing of Chinese natural speech stimuli may be related to the inherent lateralization patterns within the human brain. These states, characterized by left-lateralized and right-lateralized regions predominantly engaged in higher-order cognitive processes, exhibited heightened activity during the Chinese natural listening task.

Furthermore, the statistical analyses using linear mixed-effects models revealed that the temporal properties of the state which is similar to State 2 identified during the Chinese natural speech task were significantly higher in females than in males (for occurrence rate, t=3.0, p=2.5×10^{-3}; for mean dwell time, t=3.3, p=1.2×10^{-3}). This suggests that the temporal properties of the dynamic lateralization states observed in both the resting state and during the processing of Chinese natural speech stimuli are similar.

Validation analysis

To rule out the potential impacts of varying time window lengths on our dynamic lateralization results, we assessed the reproducibility of the DLI findings using two additional time window lengths, 18 TR and 25 TR. We consistently identified two distinct dynamic lateralization states (Fig. S4). Moreover, the two states identified using 18-TR and 25-TR time windows were both remarkably similar to those identified with the 20-TR time window (18 TR: for State 1, r=0.99, p<1.0×10^{-15}; for State 2, r=0.99, p<1.0×10^{-15}; 25 TR for State 1, r=0.99, p<1.0×10^{-15}; for State 2, r=0.99, p<1.0×10^{-15}). These results demonstrate the robustness and reliability of the DLI analysis, confirming that our results can be replicated regardless of the chosen time window length.

Discussion

In this study, we investigated the dynamic nature of whole-brain lateralization during Chinese language processing and explored the potential influences of sex and content (emotional or rational contents), as well as the genetic underpinnings of the observed dynamic lateralization. Remarkably, our findings revealed the existence of two distinct dynamic lateralization states. While the language system was predominantly found in the left hemisphere, intriguingly, we observed converse lateralization patterns for both high-order areas and primary functioning areas. These two states, associated with higher-order functioning systems exhibiting left- or right-lateralization, corresponded to the processing of rational and emotional contents, respectively. More interestingly, males displayed a pronounced inclination for the former state, while females consistently exhibited a preference for the latter state, especially during the processing of rational content. Furthermore, our investigation revealed genetic evidence that supports these observed sex differences in language processing.

First, our study revealed that, for both dynamic lateralization states, brain regions associated with language systems, such as covert and overt reading, were consistently located in the left hemisphere. This emphasized the crucial role of the left hemisphere during language processing[41-43]. However, the most notable distinction between these two states is the lateralization patterns of higher-order cognitive systems that assist in language processing in real-life scenarios. Specifically, in State 1, brain regions associated with higher-order functions such as reward processing, theory of mind, and emotion showed left lateralization. Conversely, in State 2, the brain regions involved in higher-order cognitive processes such as reward processing, theory of mind, and flanker tasks exhibited right lateralization. These findings are supported by prior studies suggesting a coordinated effort between both brain hemispheres during language comprehension[44,45]. Furthermore, our findings suggest that interhemispheric coordination during language processing is primarily due to the dynamic switching of higher-order cognitive function systems between left and right lateralization patterns, which supports the stable, left-lateralized language system.

Second, we explored the relationship between the sentiment of Chinese natural speech stimuli and the two dynamic lateralization states. Our results revealed that State 1 was strongly associated with the processing of rational content, whereas State 2 was associated with the processing of emotional content. This observation aligns with prior studies on the brain lateralization of general cognitive functions, which suggest that the left hemisphere is predominantly related to mathematical and logical reasoning[46-48], while the right hemisphere is related to emotion processing[49,50]. Consequently, we infer that during real-life language comprehension, State 1, with shows increased left lateralization for higher-order cognitive functions, likely plays a role in processing rational language components. In contrast, State 2, characterized by enhanced right lateralization for higher-order cognitive functions, appears to be associated with the interpretation of emotional language elements. Our findings, when viewed according to the related text sentiment, emphasize the distinct roles of these two states in language comprehension.

Third, we observed noteworthy sex differences in language processing, and these disparities were influenced by the type of content (emotional or rational). Irrespective of the content type, females consistently exhibited a preference for State 2, characterized by higher-order functions with more right lateralization, as evidenced by significantly higher occurrence rates and a greater inclination to transition towards this state. In contrast, males displayed a

pronounced inclination for State 1, characterized by higher-order functions with more left lateralization, particularly during the processing of rational content. These findings align with previous research on sex differences in brain lateralization during language processing, indicating a tendency for left-hemisphere engagement in males and right-hemisphere engagement in females[26-28,33,51]. More interestingly, building upon our prior conclusions regarding the distinct roles of these two states in language processing (i.e., State 1 being associated with rational content and State 2 with emotional content), we suggest that during real-life language processing, females tend to employ a perceptual thinking approach, while males tend to employ rational thinking styles. This intriguing inference aligns with the empathizing-systemizing theory, which suggests that females typically demonstrate greater empathy, while males exhibit a preference for systems-oriented approaches[25,52,53].

Fourth, the gene set enrichment analysis based on the two dynamic lateralization states elucidates their potential genetic basis. In addition to their associations with mental disorders and cognitive functions, a prominent distinction between these states was observed: in State 1, genes associated with male sex hormones, such as male-pattern baldness, were enriched, whereas in State 2, genes associated with female sex hormones, such as menarche and breast cancer, were enriched. These findings are consistent with our other results that males were more inclined towards State 1, while females consistently preferred State 2 (Fig. 4). This offers an additional genetic-level explanation for the sex disparities observed in the two lateralization states. Furthermore, these results demonstrate the potential relationship among sex differences, sex hormones, and language-related brain lateralization. These findings are supported by prior research emphasizing the substantial impact of sex hormones on language development[54-57]. Additionally, previous studies have indicated the role of biological sex and sex hormones in shaping functional cerebral asymmetries, including language lateralization[58,59]. Our findings suggest that sex differences in language lateralization may be mediated by sex hormones, which are influenced by genetic factors.

Finally, our findings elucidate the origin of the two dynamic lateralization states observed during the processing of Chinese natural speech stimuli. The results suggest that these states may originate from inherent lateralization patterns in the human brain, as previously identified in a study by Wu et al.[24]. Our results offer a novel perspective, suggesting that during language processing, the activities of these two states, characterized by left-lateralized and right-lateralized regions primarily engaged in higher-order cognitive processes, are heightened.

However, it is important to acknowledge some limitations of our study. First, the sample size was relatively small, with only 20 participants included in the analyses. Nevertheless, we attempted to mitigate this limitation by acquiring 20 scans for each participant to simulate different language contexts that occur in daily life and to increase the effective sample size. Additionally, we made efforts to achieve sex balance by recruiting 10 female participants. Future studies with larger and more diverse samples would validate our findings. Another limitation is that our study included a population of younger individuals with high-level education backgrounds (mean age 23.7 ± 1.8 years). It would be valuable to investigate the dynamic lateralization states during Chinese language processing in participants of different ages, including children and older adults. This would allow us to explore potential age-related changes in lateralization patterns and their implications for language processing. Furthermore, our analyses were specifically based on the Chinese language. It would be interesting and

important to investigate dynamic lateralization states during English language or other language processing to examine the generalizability of our findings across different linguistic contexts.

In conclusion, our study provides valuable insights into the dynamic nature of brain lateralization during Chinese language processing. The identification of two distinct lateralization states improves our understanding of interhemispheric coordination during language processing, emphasizing the dynamic shift in higher-order cognitive functions between left and right lateralization patterns. Furthermore, the associations of these lateralization states with sex differences and the processed content (emotional or rational content) offer insights into sex-specific patterns in language processing. Moreover, our genetic-level analyses suggest that the observed sex differences in language lateralization may be influenced by sex hormones. Future research should focus on replicating and expanding our findings utilizing larger and more diverse sample populations, exploring different age groups, and investigating the functional significance of the observed dynamic lateralization states. This would advance our understanding of language processing mechanisms and their relevance in clinical and cognitive contexts.

Materials and methods

Participants and task-based fMRI dataset

Fully informed consent was obtained from all participants by Fudan University, and the research procedures and ethical guidelines were approved by the Fudan University institutional review board. The task-based fMRI data were collected from a total of 20 participants (mean age 23.7 ± 1.8 years, 10 females). All participants were healthy and had normal hearing. The participants were postgraduate students with the same educational level. The task-based fMRI data were acquired using an ultrahigh-field 7T Siemens Terra MR scanner at the Zhangjiang International Brain Imaging Centre (ZIC) of Fudan University, Shanghai, China. A 32-channel Siemens volume coil (Siemens Healthcare) was used for data acquisition. Functional scans were obtained using an echo planar imaging (EPI) sequence with the following parameters: repetition time (TR) = 1,500 ms, echo time (TE) = 25 ms, flip angle = 65°, voxel size = 1.5×1.5×1.5 mm, matrix size = 128×128, field of view (FOV) = 1,920×1,920 mm, slice thickness = 1.5 mm, and number of slices = 96. The T1-weighted anatomical data were collected on a 3T scanner with the following parameters: TR = 2,500 ms, TE = 2.22 ms, flip angle = 8°, matrix size = 300×320, FOV = 240×256 mm, slice thickness = 0.8 mm, and number of slices = 208.

Data preprocessing

Image preprocessing was performed using Statistical Parametric Mapping-12 (SPM12; http://www.fil.ion.ucl.ac.uk/spm). To ensure T1 equilibrium, several volumes were not recorded prior to the trigger. The volumes were temporally realigned to the middle EPI volume and spatially realigned to correct for head movement. The structural images of each participant were registered to the mean EPI image, segmented, and normalized to Montreal Neurologic Institute (MNI) space. The realigned EPI volumes were then normalized to MNI space using deformation field parameters obtained from the structural image normalization. Finally, the normalized EPI volumes were spatially smoothed using a 6×6×6 mm Gaussian kernel and high-pass filtered to reduce noise. After preprocessing, the cortical grey matter was parcellated into 426 regions, including 360 cortical areas and 66 subcortical areas, using the HCPex atlas[37]. The

HCPex atlas is a modified and extended version of the surface-based Human Connectome Project-MultiModal Parcellation atlas of human cortical areas (HCP-MMP v1.0)[60]. This atlas provides a detailed and multimodal parcellation of brain regions, enabling the examination of dynamic lateralization in different brain regions. For each participant, time series were extracted by calculating the mean signal of all voxels within each of the 426 brain regions.

Chinese natural speech stimuli

In the task, a set of twenty 8- to 12-minute articles were utilized as the Chinese natural speech stimuli. These articles covered a wide range of genres, including fairy tales, fables, novels, essays, news, and scientific essays. A detailed summary of each article is presented in Table S1. Each article was presented during a separate fMRI scanning session; thus, a total of 20 sessions were conducted for each participant. The duration of each scan was customized to match the length of the corresponding article and included a period of silence lasting 2 seconds both before and after the article was presented. The 20 fMRI scans were conducted on different days, with a total of approximately 162 minutes of scanning time. The articles were played to participants using Sensimetrics S14 in-ear piezoelectric headphones.

Classification of Chinese natural speech stimuli

Data-driven techniques incorporating natural language processing techniques and the hierarchical clustering algorithm were employed to classify the Chinese natural speech stimuli. The NLP techniques applied in this analysis included the "Jieba" Chinese text segmentation system and text vectorization. First, Chinese word segmentation was performed using the *Jieba* word segmentation tool (https://github.com/fxsjy/jieba/). This tool divided continuous sentences into words. Next, each word was represented as a 300-dimensional numerical vector based on pretrained Chinese word vectors[61]. These vectors were trained with rich context features (word, ngram, and character) and large corpora, including Baidu Encyclopedia, Wikipedia_zh, Wikipedia_zh, Sogou News, Financial News, Zhihu_QA, Weibo, and Literature. This training produced accurate word representations in a high-dimensional semantic space. Subsequently, each article was represented as the term frequency-inverse document frequency (TF-IDF) weighted sum of the embedding vectors corresponding to each word. The TF-IDF is a statistical method that calculates the significance of a token or word to a document within a set of documents[62]. The TF-IDF score combines the term frequency (TF) and inverse document frequency (IDF). The TF, $\mathrm{tf}(t,d)$, measures how many times a token or word appears in a document:

$$\mathrm{tf}(t,d) = \frac{f_{t,d}}{\sum_{t' \in d} f_{t',d}},$$

where $f_{t,d}$ is the number of times word t occurs in document d, and the sum of $f_{t',d}$ represents the total number of words in document d.

The IDF measures how frequent or rare a token is within the entire document set:

$$\mathrm{idf}(t,D) = \log \frac{N}{|\{d \in D : t \in d\}|}$$

where N is the total number of documents and $|\{d \in D : t \in d\}|$ denotes the number of documents in which the word appears.

By multiplying these two metrics, a TF-IDF score is obtained for each word in a document:

$$\text{tf-idf}(t,d,D) = \mathrm{tf}(t,d) \cdot \mathrm{idf}(t,D)$$

Finally, the hierarchical clustering algorithm[63] was applied to the set of 20 vectorized articles. In this algorithm, the Euclidean distance and inverse squared distance (i.e., minimum variance algorithm) are utilized to calculate the distances between clusters. The clustering results were visualized using a dendrogram. The optimal number of clusters was determined by considering both the structure of the dendrogram and the silhouette criterion[36]. The clustering labels obtained with this classification algorithm were then used to investigate differences in dynamic lateralization when processing different types of Chinese natural speech stimuli.

Dynamic laterality index

To assess the dynamic brain lateralization during the processing of Chinese natural speech stimuli, we utilized a approach proposed by Wu et al.[24] for measuring the synchronization changes of brain regions in the left or right hemisphere while performing cognitive functions over time. We used a sliding window method with the window length set as 20 TR and the step set as 1 TR and calculated the dynamic laterality index for each region. For each sliding window, the DLI is defined as:

$$DLI_i = r(ROI_i, GS_L) - r(ROI_i, GS_R),$$

where ROI_i denotes the BOLD time series of ROI i, and GS_L and GS_R denote the mean global signal (GS), i.e., the BOLD time series averaged across all voxels, of all regions within the left and the right hemispheres. The Pearson correlation coefficient r is Fisher-z-transformed. To test the reproducibility of the DLI, we also employed two other window lengths to evaluate the impact of the window length on the DLI results.

To quantify the magnitude of the time-varying laterality, we measured the LF, which is defined as the standard deviation of the laterality time series[24], of each ROI for every participant.

Identification of dynamic lateralization states

To identify recurring whole-brain dynamic lateralization states, a two-stage temporal clustering approach was employed. In the first stage, we focused on individual-level analysis. For each participant, a temporal similarity matrix was computed across the total 6,114 time windows of the 20 sessions. The temporal similarity was measured as the Pearson correlation between each pair of whole-brain dynamic lateralization states in the different time windows. Then, we applied the Louvain community detection algorithm[38] to the temporal similarity matrix of the 6,114 dynamic lateralization time windows for each participant to generate clusters. The γ parameter was set to 1 in the community detection process, and the algorithm was stopped when the modularity Q no longer improved (i.e., improvement $< 1.0\times10^{-100}$), ensuring the best cluster partitioning. Each cluster represented a dynamic lateralization state at the individual level, and the state centroids (i.e., the mean of whole-brain dynamic lateralization state within a cluster) were calculated.

In the second stage, we focused on group-level analysis. To obtain group-level recurring dynamic lateralization states, a temporal similarity matrix was computed using the state centroids from all participants. The Louvain community detection algorithm was applied to analyse this matrix. Based on the group-level clustering results, all the dynamic lateralization time windows of all participants were reclassified accordingly.

Mapping text sentiment to dynamic lateralization states

Audio text segmentation and sentiment labelling. The audio data were segmented into sentences using NLP techniques. Regular expression operations were employed to identify sentence boundaries in the audio transcriptions, followed by manual correction. A group of four participants (two females and two males) was recruited to assign sentiment labels to the sentences. These participants were evenly distributed between sexes and were not involved in the task-based fMRI scanning. They rated the sentiment of each sentence, distinguishing between emotional (marked as 1) and rational (marked as 0) sentences. The sentiment ratings provided by the four participants were then averaged to obtain a sentiment score for each sentence. Moreover, we determined the sentiment score of each individual Chinese character within the sentences according to the score of that sentence.

Mapping audio texts to functional brain imaging windows. The time windows defined in the task-based fMRI data and the corresponding sections of the audio data were aligned by synchronizing the timestamps of the fMRI data with the timestamps associated with each sentence in the audio data. This temporal alignment enabled precise correspondence between the linguistic information and the neural activity captured in each window.

Calculation of sentiment scores for dynamic lateralization states. We collected the Chinese characters in the audio data for each time window in the task-based fMRI data. Subsequently, the sentiment score for each time window was computed by averaging the scores of all Chinese characters within the window, which served as a measure of the emotion of the content conveyed by the audio data during that particular window. Moreover, to minimize the influence of individual differences on the lateralization state, we determined the lateralization state of each time window by measuring the mode across the 20 participants. This approach established a relationship between the content emotions (emotional or rational) in the audio texts and the corresponding dynamic lateralization states.

Spatial properties of dynamic lateralization states

Community structure of each state. To investigate the spatial organization of the dynamic lateralization states, we first extracted the lateralization time series for each state. The lateralization time series for each state were obtained by concatenating the data from the 20 scanning sessions of the 20 participants. Subsequently, we calculated a spatial similarity matrix (426×426) based on the lateralization time series across the entire brain for each state. The similarity between regions was estimated using the Pearson correlation coefficient, and only relationships with positive weights were retained. Next, we employed the Louvain community detection algorithm[38] to determine the community structure of each dynamic lateralization state based on the spatial similarity matrix. During the community detection process, we set the parameter γ to 1, and the algorithm iterations were stopped the modularity Q no longer improved (i.e., improvement $<1.0\times10^{-100}$) to obtain the best community partitioning results. To ensure comparability among communities across different dynamic lateralization states, we aligned the communities by relabelling them according to their anatomical locations.

Additionally, we calculated the mean DLI and mean activation values of the communities for each state. Because the language listening task was a continuous process without contrasting tasks, we set the activation threshold as the mean BOLD signal value across the whole brain at each time point. The activation value for each brain region was obtained by thresholding the BOLD signal values.

Community segmentation and integration during state transitions. To quantify the process of community change during state transitions, we introduced a community transition rate (CTR) matrix that captures the segmentation and integration of communities during state transitions. Assuming a state space S, the CTR matrix from state i with M communities to state j with N communities is defined as:

$$CTR^{ij} = \begin{pmatrix} T_{11}^{ij} & T_{12}^{ij} & \cdots & T_{1N}^{ij} \\ T_{21}^{ij} & T_{22}^{ij} & \cdots & T_{2N}^{ij} \\ \vdots & \vdots & \ddots & \vdots \\ T_{M1}^{ij} & T_{M2}^{ij} & \cdots & T_{MN}^{ij} \end{pmatrix}, \ i,j \in S.$$

Here, T_{mn}^{ij} represents the (m,n) element of CTR^{ij}, given by:

$$CTR^{ij}(m,n) = T_{mn}^{ij} = \frac{NR_{mi}}{NR_{nj}}, m = 1,2,\cdots,M \ and \ n = 1,2,\cdots,N.$$

where NR_{mi} represents the number of brain regions in the mth community in state i, and NR_{nj} represents the number of brain regions in the nth community in state j. Since the matrix elements represent transition rates, they must satisfy:

$$0 \leq CTR_{ij}(m,n) \leq 1.$$

Furthermore, as the brain regions in a community in one state must be allocated to one of the available communities in another state, the transition matrix must satisfy:

$$\sum_{n=1}^{N} CTR_{ij}(m,n) = 1, \text{ for all } m.$$

Temporal properties of dynamic lateralization states

Occurrence rate and mean dwell time. The temporal properties of the dynamic lateralization states were assessed using the occurrence rate and mean dwell time[64,65]. The occurrence rate represents the proportion of time windows spent in each dynamic lateralization state, measured as a percentage. The mean dwell time indicates the duration of time that a participant remains in a specific dynamic lateralization state, calculated by averaging the number of consecutive windows spent in that state before transitioning to another state.

Transition probability. To characterize the transitions between brain states, we estimated the transition probability matrix using the dynamic lateralization state time series for each participant and scanning session. Assuming a state space S with N brain states, the estimated transition probability matrix for the dynamic lateralization state series is denoted as $P\ (N \times N)$. The element (i,j) in matrix P is calculated as:

$$p_{ij} = \frac{n_{ij}}{\sum_j n_{ij}}, i,j \in S$$

where n_{ij} denotes the number of times state i transitions to state j.

Statistical analysis

We employed linear mixed-effects models[66] to investigate the potential effects of the temporal properties of the dynamic lateralization states, with age and the number of time windows as covariates in the analysis.

Differences in the temporal properties between states. We compared the differences in the occurrence rate among different states using the following model:

$$occurrence\ rate \sim state + (1|subject\ ID) + (1|sex) + (1|content\ types).$$

This model included fixed effects for brain lateralization states and random effects for participants, sex, and content types since the task employed a within-subject design. To assess

the significance of the explanatory variable in the mixed-effects model, we performed N = 10000 permutations of the response variable. Additionally, we evaluated the differences in the mean dwell time among different states using the same model.

Differences in the transition probabilities between transition directions. We compared the differences in the transition probability between different the two transition directions (i.e., States 1 to 2 or States 2 to 1) using the following model:

$$transition\ probability \sim transition\ direction + (1|subject\ ID) + (1|sex) + (1|content\ types).$$

A permutation test (N = 10000) was performed to determine the significance of the mixed-effects model.

Differences in the temporal properties between sexes or content types. We compared the differences in the occurrence rate between different conditions (sexes or content types) using the following model:

$$occurrence\ rate \sim condition + (1|subject\ ID).$$

We performed a permutation test (N = 10000) to assess the significance of the mixed-effects model. Similarly, the differences in the mean dwell time (or transition probability) between sexes or content types were assessed using the same approach.

Differences in the laterality fluctuation between sexes or content types. We compared the differences in the laterality fluctuation between different conditions (sexes or content types) using the following model:

$$laterality\ fluctuations \sim condition + (1|Subject\ ID).$$

The linear mixed-effects model was fitted for the LF value of each brain region. P values were corrected for multiple comparisons using Benjamini–Hochberg false discovery rate (BH-FDR) corrections (q value < 0.05)[67].

Gene expression analysis of dynamic lateralization states

Gene expression data. Regional microarray expression data were obtained from six postmortem brains (one female, ages 24.0~57.0 years, mean age 42.50±13.38 years) provided by the Allen Human Brain Atlas (AHBA, https://human.brain-map.org)[68]. The data were processed using the abagen toolbox (version 0.1.3; https://github.com/rmarkello/abagen) and the HCPex atlas, a 426-region volumetric atlas in MNI space.

First, the microarray probes were annotated using the data provided by Arnatkevičiūtė et al.[69]. The probes that did not match a valid Entrez ID were discarded. Next, the probes were filtered based on their expression intensity relative to background noise[70]. Probes with intensities lower than the background in >=50.00% of samples across donors were discarded. In cases where multiple probes matched the expression of the same gene, we selected the probe with the most consistent pattern according to regional variations across donors (i.e., differential stability)[71]. The differential stability was calculated using the formula:

$$\Delta_S(p) = \frac{1}{\binom{N}{2}} \sum_{i=1}^{N-1} \sum_{j=i+1}^{N} \rho\left[B_i(p), B_j(p)\right],$$

where ρ is the Spearman's rank correlation of the expression of a single probe, p, across regions in two donors B_i and B_j, and N is the total number of donors. The regions corresponded to the structural designations provided in the ontology from the AHBA.

The MNI coordinates of the tissue samples were updated by performing nonlinear registration using advanced normalization tools (ANTs; https://github.com/chrisfilo/alleninf).

Samples were assigned to brain regions in the provided atlas if their MNI coordinates were within 2 mm of a given parcel. To minimize assignment errors, sample-to-region matching was constrained by hemisphere and gross structural divisions (i.e., cortex, subcortex/brainstem, and cerebellum). For example, a sample in the left cortex could be assigned only to an atlas parcel in the left cortex[69]. If a brain region was not assigned a sample from any donor based on the above procedure, the tissue sample closest to the centroid of that parcel was identified independently for each donor. The average of these samples, weighted by the distance between the parcel centroid and the sample, was calculated across donors to estimate the parcellated expression values for the missing region. Tissue samples that were not assigned to a brain region in the provided atlas were discarded.

To address intersubject variation, tissue sample expression values were normalized across genes using a robust sigmoid function[72]:

$$x_{norm} = \frac{1}{1 + \exp(-\frac{(x - \langle x \rangle)}{\mathrm{IQR}_x})},$$

where $\langle x \rangle$ is the median and IQR_x is the normalized interquartile range of the expression of a single tissue ample across genes. Normalized expression values were then rescaled to the unit interval:

$$x_{scaled} = \frac{x_{norm} - min(x_{norm})}{max(x_{norm}) - min(x_{norm})}.$$

The gene expression values were normalized across tissue samples using the same procedure. Samples assigned to the same brain region were averaged separately for each donor and then across donors. The fully preprocessed gene data included a 426 by 15632 matrix of microarray gene expression data.

Identification of genes correlated with dynamic lateralization states. We performed correlation analyses between each group-averaged dynamic lateralization state and the Allen Human Brain spatial gene expression patterns. For each dynamic lateralization state, we calculated the Pearson correlation between each 426-region gene expression vector and the 426-region dynamic lateralization state vector. Multiple comparisons were corrected using BH-FDR corrections (q value < 0.05). Genes that exhibited significant correlations with lateralization states were identified as dynamic lateralization-related genes.

Gene set enrichment analysis. To provide further biological insights into the genes that exhibited significant correlations with the lateralization states, we conducted gene set enrichment analysis (GSEA) with FUMA, an integrative web-based platform[73]. We employed the GENE2FUNC function to evaluate the enrichment of the dynamic lateralization-related genes. In the enrichment analysis, hypergeometric tests were performed to determine if the mapped genes were overrepresented in any of the predefined gene sets. Gene sets were obtained from the genes reported in the GWAS Catalog[40]. Multiple test correction was conducted using BH-FDR corrections with an adjusted P value cut-off of 0.05 and a minimum of 2 overlapping genes.

Comparison of dynamic lateralization states identified during the resting state and the processing of Chinese natural speech stimuli

The dynamic brain lateralization was analysed using resting-state fMRI data collected from a sample of 991 participants enrolled in the HCP cohort. Detailed algorithm parameters can be

found in a previous study[24]. We quantified the similarity between the group-averaged dynamic lateralization states observed during the Chinese natural listening task and those observed during the resting state.

Furthermore, we statistically analysed the temporal properties of the dynamic lateralization states identified during the resting state, including the occurrence rate and mean dwell time. To investigate potential disparities in these temporal properties between sexes, we employed the following linear mixed-effects model, with age, education level, race, and grey matter volume (GMV) as covariates and the family ID as a random effect:

$$occurrence\ rate/mean\ dwell\ time \sim sex + age + education + race + GMV + (1|family\ ID).$$

Acknowledgements

This work was supported by the Natural Science Foundation of China (grant numbers 81901826, 61932008, 62076068, 82271627), the Natural Science Foundation of Shanghai (grant numbers 19ZR1405600, 20ZR1404900), the National Key R&D Program of China (grant numbers 2018YFC1312900 and 2019YFA0709502) the Shanghai Municipal Science and Technology Major Project (grant number 2018SHZDZX01), the ZJ Lab, Shanghai Center for Brain Science and Brain-Inspired Technology and the 111 Project (grant number B18015), and the National Science and Technology Council (Taiwan, grant number NSTC 112-2221-E-033-019).

Authors' contributions

All authors had full access to the data in the study and accepted the responsibility to submit it for publication. M.C. and J.F. proposed the study. R.Z. analysed the data. S.G. and W.G. prepared the experimental materials and collected the fMRI data. S.G. preprocessed the data. X.W. and X.Z. assisted in the data analysis. R.Z., M.C., J.F., J.L., X.C., and J.Z. contributed to the interpretation of results. R.Z. and M.C. drafted the manuscript. R.Z. and M.C. edited the manuscript. R.Z. contributed to visualization. All authors approved the manuscript.

Code availability

Python 3.9.7 was utilized for the analysis of audio texts using natural language processing (NLP) techniques. The NLP techniques applied in this study included the "Jieba" Chinese text segmentation system (https://github.com/fxsjy/jieba/) and text vectorization (https://github.com/Embedding/Chinese-Word-Vectors). Gene expression data were processed in Python using the abagen toolbox (version 0.1.3; https://github.com/rmarkello/abagen). MATLAB 2018b was utilized to calculate the whole-brain dynamic laterality index (DLI) and perform statistical analyses. The MATLAB Brain Connectivity Toolbox (https://sites.google.com/site/bctnet/) was used to perform community detection based on the whole-brain DLI values to identify the dynamic lateralization states and spatial communities of the states. In addition, the MATLAB functions "linkage" and "fitglme" were utilized for the hierarchical clustering of the vectorized articles processed through NLP techniques and for the implementation of the linear mixed-effects models, respectively.

Competing interests

The authors declare no conflict of interest related to this work.

Figures

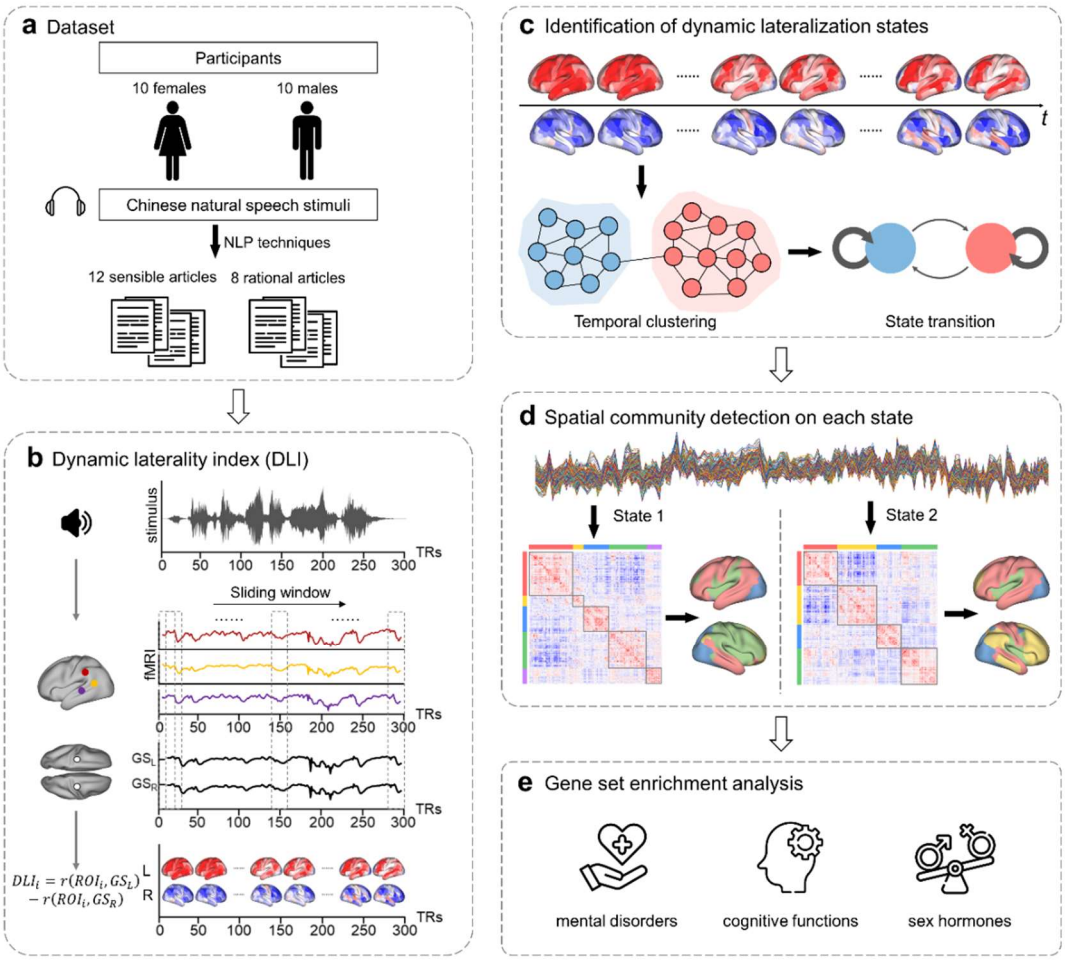

Fig. 1 Overview of the study. Panel **a** presents task-based fMRI data acquired from a total of 20 participants, including 10 females. Participants were presented with a series of twenty 8- to 12-minute articles, which were categorized into two groups (12 emotional articles and 8 rational articles) using NLP techniques and a hierarchical clustering algorithm. Panel **b** illustrates the definition of the DLI. The DLI of ROI_i within the time window t is defined as the correlation coefficient (z-transformed) between GS_L and the ROI minus the correlation coefficient between GS_R and the ROI. Using a sliding window approach, we obtained a DLI time series for each ROI. Panel **c** shows the temporal clustering of the whole-brain lateralization patterns, which identifies recurring dynamic lateralization states. Panel **d** depicts the spatial clustering results of the dynamic lateralization states, which identified spatial communities. Panel **e** shows the gene set enrichment analysis of the dynamic lateralization states.

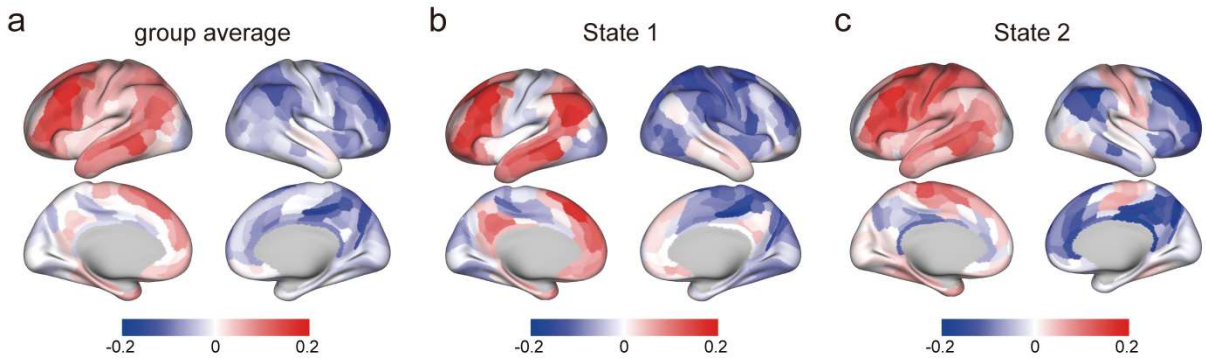

Fig. 2 Identification of two dynamic lateralization states. Panel **a** presents the group-averaged lateralization maps across all time windows, with the majority of brain regions in both hemispheres consistently showing lateralization towards the corresponding side. Panel **b** shows State 1 of the two dynamic lateralization states, where the left hemisphere exhibited strong left lateralization in regions such as the dorsolateral prefrontal cortex and inferior parietal cortex (such as area 45). Panel **c** displays State 2 of the two dynamic lateralization states, with the right hemisphere displaying pronounced right lateralization in the dorsolateral prefrontal cortex, posterior cingulate cortex, and inferior parietal cortex. Panels **b** and **c** depict a distinct reversal in the lateralization pattern of specific brain regions between State 1 and State 2, including the somatosensory cortex, the paracentral lobule, and the middle cingulate cortex. In State 1, these regions in the left hemisphere exhibited right lateralization, whereas in State 2, these same regions within the right hemisphere displayed left lateralization.

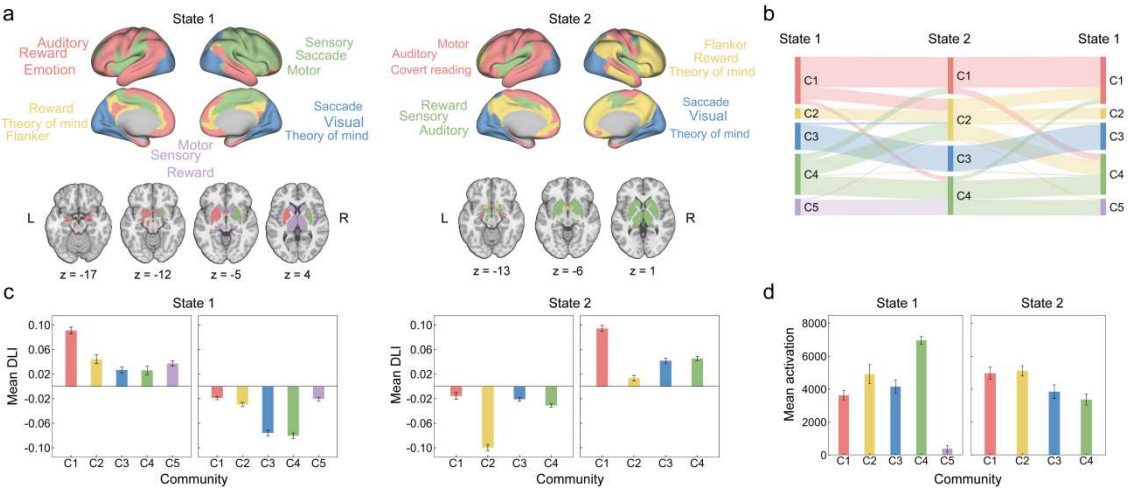

Fig. 3 Spatial organization of dynamic lateralization states. Panel **a** shows the community structures within the two dynamic lateralization states. State 1 exhibits the presence of five distinct spatial communities, and State 2 presents four spatial communities. Panel **b** illustrates the segmentation and integration of the communities during the state transitions. Panel **c** presents the mean DLI values for the communities in these two states. Panel **d** displays the mean activation values for the communities in these two states. The error bars in panels **c** and **d** denote the mean ± SEM.

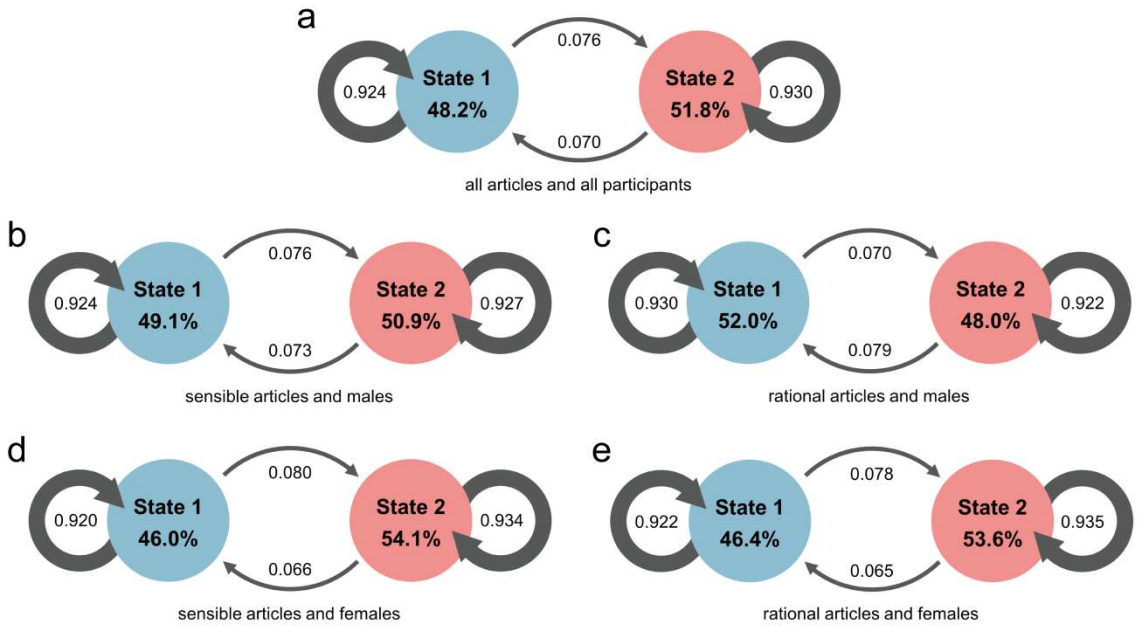

Fig. 4 Temporal properties of dynamic lateralization states. Panel **a** shows the occurrence rates and the mean dwell times of the two states, as well as the transition probabilities between states across all participants and all article sessions. Panels **b** to **e** depict these temporal properties for different sexes and content types. Linear mixed-effects models were employed to investigate their potential effects on these temporal properties, with age and the number of time windows as covariates in the analysis. The significance of the mixed-effects models was assessed by permutation tests (N = 10000).

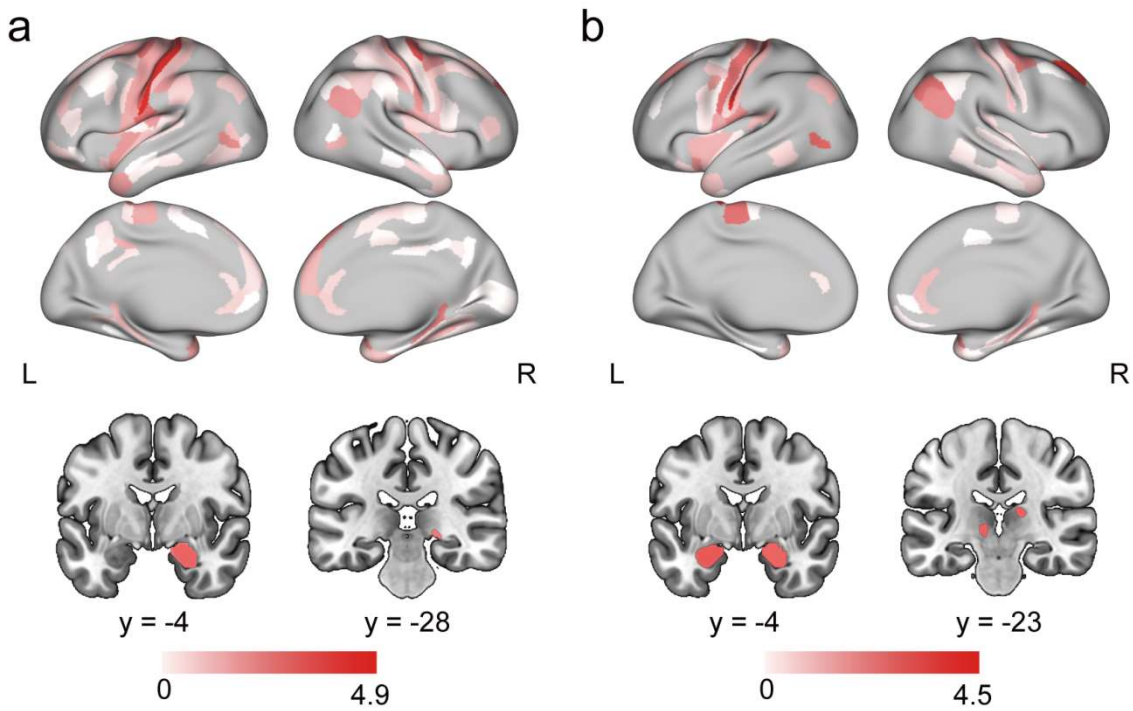

Fig. 5 Differences in the laterality fluctuation between sexes (males > females) during the processing of articles with rational content. Panels **a** and **b** display brain regions exhibiting significant differences in laterality fluctuation in State 1 and State 2, respectively. The statistical analyses were conducted using linear mixed-effects models, with age and the number of time windows as covariates. The linear mixed-effects model was fitted according to the LF of each brain region using BH-FDR corrections for multiple comparisons (q value < 0.05).

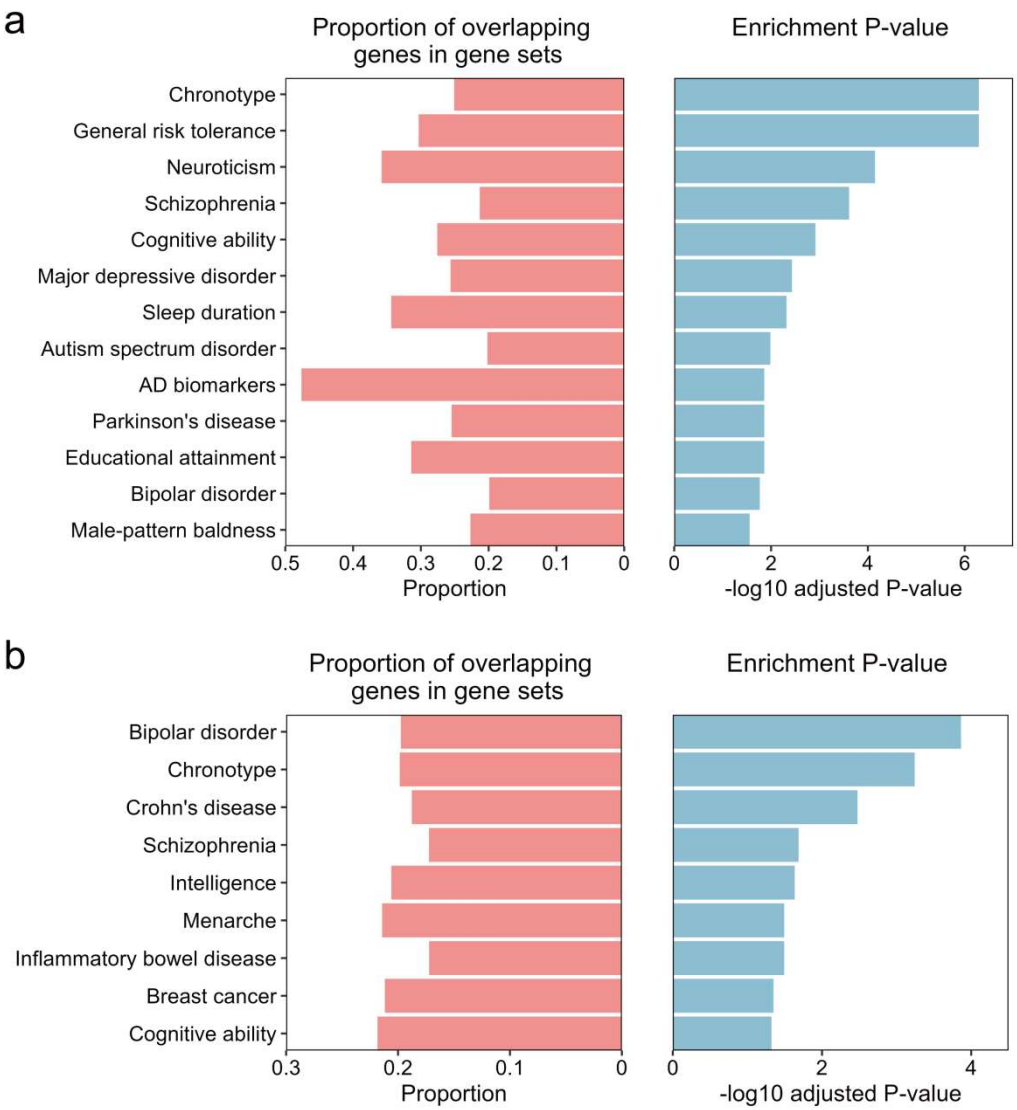

Fig. 6 Gene set enrichment analysis for genes associated with dynamic lateralization states. Panels a and b display the biological functions associated with the genes related to the two dynamic lateralization states, as retrieved from the GWAS Catalogue. Multiple test correction was conducted using BH-FDR corrections, with an adjusted P value cut-off of 0.05 and a minimum of 2 overlapping genes.

Tables

Table 1 Two categories of the Chinese natural speech stimuli

No.	Title	Genre	Category
1	The Rabbit Who Went to the Moon	fairy tale	emotional
2	Severing the Friendship	fable	emotional
3	The Family	novel	emotional
4	The Class Adviser	novel	emotional
5	The Color of Light	essay	emotional
6	The Hometown Banyan Trees	essay	emotional
7	Police Arrest 26 Suspects After Airing of "Crazy Personal Information Black Market"	news	rational
8	Huabei Connects to the Central Bank's Credit System, Gradually Covering All User Groups	news	rational
9	Petroleum Resources	scientific explanatory essay	rational
10	Bombed by Negative News, Here's How to Maintain Mental Health	news	rational
11	School in the Clouds	fairy tale	emotional
12	The Battle of the Yellow Emperor Against Chi You	fable	emotional
13	Chronicle of a Blood Merchant	novel	emotional
14	Ordinary World	novel	emotional
15	Poetic Night Rain	essay	emotional
16	The Five Key Flavors of Chinese Food	essay	emotional
17	Safeguarding the Vital Thread of Ethnic Unity	news	rational
18	Chinese President Xi Jinping Empowers Entrepreneurs for Greater Economic Impact	news	rational
19	Flowing Water on Mars	scientific explanatory essay	rational
20	How Does the Brain Perceive the Passage of Time?	scientific explanatory essay	rational

References

1 Vallortigara, G., Chiandetti, C. & Sovrano, V. A. Brain asymmetry (animal). *Wiley Interdisciplinary Reviews: Cognitive Science* **2**, 146-157 (2011).

2 Esteves, M., Lopes, S. S., Almeida, A., Sousa, N. & Leite-Almeida, H. Unmasking the relevance of hemispheric asymmetries—Break on through (to the other side). *Progress in neurobiology* **192**, 101823 (2020).

3 McAvoy, M. *et al.* Unmasking Language Lateralization in Human Brain Intrinsic Activity. *Cerebral Cortex* **26**, 1733-1746 (2015).

4 Lazard, D. S., Collette, J. L. & Perrot, X. Speech processing: from peripheral to hemispheric asymmetry of the auditory system. *The Laryngoscope* **122**, 167-173 (2012).

5 Gerrits, R., Verhelst, H. & Vingerhoets, G. Mirrored brain organization: Statistical anomaly or reversal of hemispheric functional segregation bias? *Proceedings of the National Academy of Sciences* **117**, 14057-14065 (2020).

6 Joliot, M., Tzourio-Mazoyer, N. & Mazoyer, B. Intra-hemispheric intrinsic connectivity asymmetry and its relationships with handedness and language Lateralization. *Neuropsychologia* **93**, 437-447 (2016).

7 Binder, J. R. *et al.* Human brain language areas identified by functional magnetic resonance imaging. *Journal of Neuroscience* **17**, 353-362 (1997).

8 Fedorenko, E., Hsieh, P.-J., Nieto-Castañón, A., Whitfield-Gabrieli, S. & Kanwisher, N. New method for fMRI investigations of language: defining ROIs functionally in individual subjects. *Journal of neurophysiology* **104**, 1177-1194 (2010).

9 Price, C. J. A review and synthesis of the first 20 years of PET and fMRI studies of heard speech, spoken language and reading. *Neuroimage* **62**, 816-847 (2012).

10 Bialystok, E., Craik, F. I., Klein, R. & Viswanathan, M. Bilingualism, aging, and cognitive control: evidence from the Simon task. *Psychology and aging* **19**, 290 (2004).

11 Novick, J. M., Trueswell, J. C. & Thompson-Schill, S. L. Broca's area and language processing: Evidence for the cognitive control connection. *Language and Linguistics Compass* **4**, 906-924 (2010).

12 Feng, G., Chen, H.-C., Zhu, Z., He, Y. & Wang, S. Dynamic brain architectures in local brain activity and functional network efficiency associate with efficient reading in bilinguals. *Neuroimage* **119**, 103-118 (2015).

13 Doron, K. W., Bassett, D. S. & Gazzaniga, M. S. Dynamic network structure of interhemispheric coordination. *Proceedings of the National Academy of Sciences* **109**, 18661-18668 (2012).

14 Federmeier, K. D., Jongman, S. R. & Szewczyk, J. M. Examining the role of general cognitive skills in language processing: a window into complex cognition. *Current directions in psychological science* **29**, 575-582 (2020).

15 Makuuchi, M. & Friederici, A. D. Hierarchical functional connectivity between the core language system and the working memory system. *Cortex* **49**, 2416-2423 (2013).

16 Fedorenko, E. & Thompson-Schill, S. L. Reworking the language network. *Trends in cognitive sciences* **18**, 120-126 (2014).

17 Peng, X. *et al.* Robust dynamic brain coactivation states estimated in individuals. *Science Advances* **9**, eabq8566 (2023).

18 Zheng, B. *et al.* Semantic and attentional networks in bilingual processing: fMRI connectivity signatures of translation directionality. *Brain and cognition* **143**, 105584 (2020).

19 Pliatsikas, C. Understanding structural plasticity in the bilingual brain: The Dynamic Restructuring Model. *Bilingualism: Language and Cognition* **23**, 459-471 (2020).

20 Wirsich, J., Giraud, A.-L. & Sadaghiani, S. Concurrent EEG-and fMRI-derived functional connectomes exhibit linked dynamics. *NeuroImage* **219**, 116998 (2020).

21 Hiltunen, T. *et al.* Infra-slow EEG fluctuations are correlated with resting-state network dynamics in fMRI. *Journal of Neuroscience* **34**, 356-362 (2014).

22 Kucyi, A., Tambini, A., Sadaghiani, S., Keilholz, S. & Cohen, J. R. Spontaneous cognitive processes and the behavioral validation of time-varying brain connectivity. *Network neuroscience* **2**, 397-417 (2018).

23 Chai, L. R., Mattar, M. G., Blank, I. A., Fedorenko, E. & Bassett, D. S. Functional network dynamics of the language system. *Cerebral Cortex* **26**, 4148-4159 (2016).

24 Wu, X. *et al.* Dynamic changes in brain lateralization correlate with human cognitive performance. *PLoS biology* **20**, e3001560 (2022).

25 Greenberg, D. M. *et al.* Sex and age differences in "theory of mind" across 57 countries using the English version of the "Reading the Mind in the Eyes" Test. *Proceedings of the National Academy of Sciences* **120**, e2022385119 (2023).

26 Clements, A. *et al.* Sex differences in cerebral laterality of language and visuospatial processing. *Brain and language* **98**, 150-158 (2006).

27 Yang, Y. *et al.* Men and women differ in the neural basis of handwriting. *Hum Brain Mapp* **41**, 2642-2655 (2020).

28 Xu, M. *et al.* Sex differences in functional brain networks for language. *Cerebral Cortex* **30**, 1528-1537 (2020).

29 Kansaku, K., Yamaura, A. & Kitazawa, S. Sex Differences in Lateralization Revealed in the Posterior Language Areas. *Cerebral Cortex* **10**, 866-872 (2000).

30 Shaywitz, B. A. *et al.* Sex differences in the functional organization of the brain for language. *Nature* **373**, 607-609 (1995).

31 Kimura, D. Cognitive function: sex differences and hormonal influence. *Neuroscience year: supplement* **2**, 41-43 (1992).

32 Levy, J. Lateral specialization of the human brain, behavioral manifestations and possible evolutionary basis. *The biology of behavior* (1972).

33 Burman, D. D., Minas, T., Bolger, D. J. & Booth, J. R. Age, sex, and verbal abilities affect location of linguistic connectivity in ventral visual pathway. *Brain and language* **124**, 184-193 (2013).

34 Labache, L., Ge, T., Yeo, B. T. & Holmes, A. J. Language network lateralization is reflected throughout the macroscale functional organization of cortex. *Nature Communications* **14**, 3405 (2023).

35 Huth, A. G., De Heer, W. A., Griffiths, T. L., Theunissen, F. E. & Gallant, J. L. Natural speech reveals the semantic maps that tile human cerebral cortex. *Nature* **532**, 453-458 (2016).

36 Rousseeuw, P. J. Silhouettes: a graphical aid to the interpretation and validation of cluster analysis. *Journal of computational and applied mathematics* **20**, 53-65 (1987).

37 Huang, C. C., Rolls, E. T., Feng, J. & Lin, C. P. An extended Human Connectome Project multimodal parcellation atlas of the human cortex and subcortical areas. *Brain Struct Funct* **227**, 763-778 (2022).

38 Blondel, V. D., Guillaume, J.-L., Lambiotte, R. & Lefebvre, E. Fast unfolding of communities in large networks. *Journal of statistical mechanics: theory and experiment* **2008**, P10008 (2008).

39 Yeo, B. T. *et al.* Functional specialization and flexibility in human association cortex. *Cerebral cortex* **25**, 3654-3672 (2015).

40 MacArthur, J. *et al.* The new NHGRI-EBI Catalog of published genome-wide association studies (GWAS Catalog). *Nucleic Acids Res* **45**, D896-D901 (2017).

41 Braga, R. M., DiNicola, L. M., Becker, H. C. & Buckner, R. L. Situating the left-lateralized language network in the broader organization of multiple specialized large-scale distributed networks. *Journal of neurophysiology* **124**, 1415-1448 (2020).

42 Budisavljevic, S. *et al.* Age-related differences and heritability of the perisylvian language networks. *Journal of Neuroscience* **35**, 12625-12634 (2015).

43 Olulade, O. A. *et al.* The neural basis of language development: Changes in lateralization over age. *Proceedings of the National Academy of Sciences* **117**, 23477-23483 (2020).

44 Fernandino, L. *et al.* Concept representation reflects multimodal abstraction: A framework for embodied semantics. *Cerebral cortex* **26**, 2018-2034 (2016).

45 Jung-Beeman, M. *et al.* Neural activity when people solve verbal problems with insight. *PLoS biology* **2**, e97 (2004).

46 Friederici, A. D. Evolution of the neural language network. *Psychonomic bulletin & review* **24**, 41-47 (2017).

47 Verhelst, H., Dhollander, T., Gerrits, R. & Vingerhoets, G. Fibre-specific laterality of white matter in left and right language dominant people. *Neuroimage* **230**, 117812 (2021).

48 Westerhausen, R., Kompus, K. & Hugdahl, K. Mapping hemispheric symmetries, relative asymmetries, and absolute asymmetries underlying the auditory laterality effect. *Neuroimage* **84**, 962-970 (2014).

49 Stoyanov, Z., Decheva, L., Pashalieva, I. & Nikolova, P. Brain asymmetry, immunity, handedness. *Central European Journal of Medicine* **7**, 1-8 (2012).

50 Watanabe, H. *et al.* Asymmetry of the endogenous opioid system in the human anterior cingulate: a putative molecular basis for lateralization of emotions and pain. *Cerebral Cortex* **25**, 97-108 (2015).

51 Packheiser, J. *et al.* A large-scale estimate on the relationship between language and motor lateralization. *Scientific reports* **10**, 13027 (2020).

52 Baron-Cohen, S., Richler, J., Bisarya, D., Gurunathan, N. & Wheelwright, S. The systemizing quotient: an investigation of adults with Asperger syndrome or high–functioning autism, and normal sex differences. *Philosophical Transactions of the Royal Society of London. Series B: Biological Sciences* **358**, 361-374 (2003).

53 Greenberg, D. M., Warrier, V., Allison, C. & Baron-Cohen, S. Testing the empathizing–systemizing theory of sex differences and the extreme male brain theory of autism in half a million people. *Proceedings of the National Academy of Sciences* **115**, 12152-12157 (2018).

54 Bowers, J. M., Perez-Pouchoulen, M., Edwards, N. S. & McCarthy, M. M. Foxp2 mediates sex differences in ultrasonic vocalization by rat pups and directs order of maternal retrieval. *Journal of Neuroscience* **33**, 3276-3283 (2013).

55 Enard, W. *et al.* Molecular evolution of FOXP2, a gene involved in speech and language. *Nature* **418**, 869-872 (2002).

56 Haesler, S. *et al.* Incomplete and inaccurate vocal imitation after knockdown of FoxP2 in songbird basal ganglia nucleus Area X. *PLoS biology* **5**, e321 (2007).

57 Wermke, K., Quast, A. & Hesse, V. From melody to words: The role of sex hormones in early language development. *Hormones and behavior* **104**, 206-215 (2018).

58 Hausmann, M. Why sex hormones matter for neuroscience: A very short review on sex, sex hormones, and functional brain asymmetries. *Journal of Neuroscience Research* **95**, 40-49 (2017).

59 Maney, D. L. Perils and pitfalls of reporting sex differences. *Philosophical Transactions of the Royal Society B: Biological Sciences* **371**, 20150119 (2016).

60 Glasser, M. F. *et al.* A multi-modal parcellation of human cerebral cortex. *Nature* **536**, 171-178 (2016).

61 Li, S. *et al.* Analogical Reasoning on Chinese Morphological and Semantic Relations. *In Proceedings of the 56th Annual Meeting of the Association for Computational Linguistics* **2**, 138–143 (2018).

62 Hakim, A. A., Erwin, A., Eng, K. I., Galinium, M. & Muliady, W. Automated document classification for news article in Bahasa Indonesia based on term frequency inverse document frequency (TF-IDF) approach. *In 2014 6th international conference on information technology and electrical engineering (ICITEE)*, 1-4 (2014).

63 Nielsen, F. *Introduction to HPC with MPI for Data Science*. (Springer, 2016).

64 Zhou, Q., Zhang, L., Feng, J. & Lo, C.-Y. Z. Tracking the main states of dynamic functional connectivity in resting state. *Frontiers in neuroscience* **13**, 685 (2019).

65 Ryali, S. *et al.* Temporal dynamics and developmental maturation of salience, default and central-executive network interactions revealed by variational Bayes hidden Markov modeling. *PLoS computational biology* **12**, e1005138 (2016).

66 Pinheiro, J. C. & Bates, D. M. Unconstrained parametrizations for variance-covariance matrices. *Statistics and computing* **6**, 289-296 (1996).

67 Benjamini, Y. & Hochberg, Y. Controlling the false discovery rate: a practical and powerful approach to multiple testing. *Journal of the Royal statistical society: series B (Methodological)* **57**, 289-300 (1995).

68 Hawrylycz, M. J. *et al.* An anatomically comprehensive atlas of the adult human brain transcriptome. *Nature* **489**, 391-399 (2012).

69 Arnatkevičiūtė, A., Fulcher, B. D. & Fornito, A. A practical guide to linking brain-wide gene expression and neuroimaging data. *Neuroimage* **189**, 353-367 (2019).

70 Quackenbush, J. Microarray data normalization and transformation. *Nature genetics* **32**, 496-501 (2002).

71 Hawrylycz, M. *et al.* Canonical genetic signatures of the adult human brain. *Nature neuroscience* **18**, 1832-1844 (2015).

72 Fulcher, B. D., Little, M. A. & Jones, N. S. Highly comparative time-series analysis: the empirical structure of time series and their methods. *Journal of the Royal Society Interface* **10**, 20130048 (2013).

73 Watanabe, K., Taskesen, E., Van Bochoven, A. & Posthuma, D. Functional mapping and annotation of genetic associations with FUMA. *Nature communications* **8**, 1826 (2017).